

## EXPERIMENTAL STUDY ON THE VALIDITY OF REAL-TIME HYBRID VIBRATION EXPERIMENTS WITH A 2-DIMENSIONAL AND 3-DEGREES-OF-FREEDOM MODEL

Hiroshi KOBAYASHI<sup>1</sup> And Keiichi TAMURA<sup>2</sup>

### SUMMARY

The real-time hybrid vibration experiment is a new concept experiment combining shaking table test and numerical response analysis in real-time. In this paper, we have integrated the freedom of control to 2-dimensional and 3-degrees and conducted the real-time hybrid vibration experiments. Results of the experiments are compared with those of conventional shaking table tests, and the validity of real-time hybrid vibration experiment is demonstrated

### INTRODUCTION

Most of the conventional hybrid experiments are pseudo dynamic experiments with an expanded time axis due to limitations of devices, e.g., capability of computation and compensation for actuator delay, and few precedents exist for hybrid vibration experiments using shaking tables. Differing from those conventional techniques, the real-time hybrid vibration experiment is a new concept experiment combining shaking table test and numerical response analysis in real-time.

We have developed a real-time hybrid experiment system at the Public Works Research Institute after the 1995 Kobe Earthquake. At the first stage of experiments, we conducted the real-time hybrid vibration experiment with a 2 degrees-of-freedom model [Tamura and Kobayashi, 1998]. This model was a 2 storied slab structure supported by rubber bearings. Presented are the results of real-time hybrid vibration experiments with a 2-dimensional and 3 degrees-of-freedom model. Results are compared with those of shaking table tests and the validity of real-time hybrid vibration experiment is demonstrated.

### OVERVIEW OF REAL-TIME HYBRID VIBRATION EXPERIMENT

As Figure 1 shows, in the real-time hybrid vibration experiment, an original structure is divided into two parts. One is an actual model specimen of original structure. This specimen is usually taken as a part of structure whose seismic behavior is unknown or complicated. The other is a numerical model for vibration response analysis. This model represents a part of structure whose seismic behavior can be evaluated by numerical analysis.

The numerical model consists of structural elements (mass, damping and stiffness matrices), external force that is calculated from the acceleration of shaking table, and reaction force generated at the boundary of the actual and numerical models. In the numerical analysis, the external and reaction forces are inputted, and the displacement of the actual model for the next time step is calculated. This displacement is realized by actuators. Then, the external and reaction forces are measured and taken into numerical analysis. Iterating these procedures, the seismic behavior of original structure can be accurately simulated.

The equation of motion for numerical analysis is described as

$$M\ddot{x} + C\dot{x} + Kx = p + q \quad (1)$$

<sup>1</sup> Asahi, Tsukuba-shi, Ibaraki-ken, Earthquake Disaster Prevention Research Center, Japan. Email: h-koba@pwri.go.jp

<sup>2</sup> Asahi, Tsukuba-shi, Ibaraki-ken, Earthquake Disaster Prevention Research Center, Japan. Email: tamura@pwri.go.jp

where

- $M$ : Mass matrix
- $C$ : Damping matrix
- $K$ : Stiffness matrix
- $x$ : Relative displacement vector
- $p$ : external force (seismic response) vector
- $q$ : reaction force vector

Using on eq. (1), the vibration response (displacement vector  $x$ ) after a short interval  $\Delta t$  is calculated from the measured reaction force vector  $q$  and the external force vector  $p$ , where central difference method is employed.

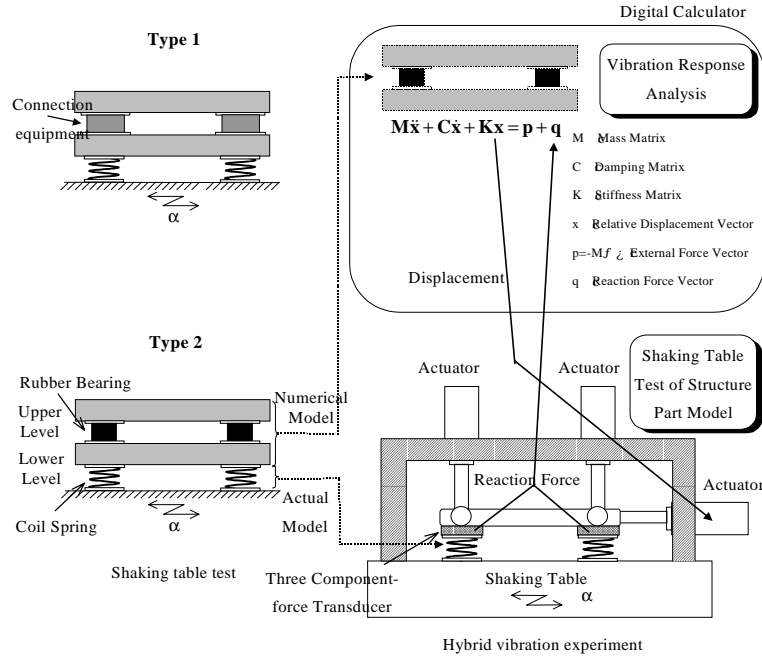


**Figure 1: Conceptual view of hybrid vibration experiment**

## FEATURES OF REAL-TIME HYBRID VIBRATION EXPERIMENT

### Vibration Response Analysis (Central Difference Method)

The central difference method is employed in vibration response analysis, because it takes short time to generate actuator signal for the next time step after measuring reaction force. An equation of motion can be written as eq.(2) at time  $t_i$ , where subscript  $i$  represents the  $i$ -th time step.

$$M\ddot{x}_i + C\dot{x}_i + Kx_i = p_i + q_i \quad (2)$$

Since the change of motion during calculation time interval  $\Delta t$  is small, we assume constant acceleration over the period between  $t_{i-1}=t_i-\Delta t$  and  $t_{i+1}=t_i+\Delta t$ , as shown in Figure 2. The displacement at  $t_{i+1}$  can be obtained from the known data at the time  $t_i$ , using eq. (3). Time required for one cycle process is 2.08ms [Umekita, et al., 1997].

$$x_{i+1} = (M + \frac{f\Delta t}{2}C)^{-1} \left\{ M(2x_i - x_{i-1}) + \frac{f\Delta t}{2}Cx_{i-1} + f\Delta t^2(p_i + q_i - Kx_i) \right\} \quad (3)$$

## Actuator Delay Compensation

Although actuator response delay has unfavorable influence on the real-time hybrid vibration experiment, it is inevitable with a hydraulic actuator. Therefore, a compensation technique is adopted. This technique predicts the displacement of an actuator at the time after actuator delay time [Horiuchi, et al., 1996].

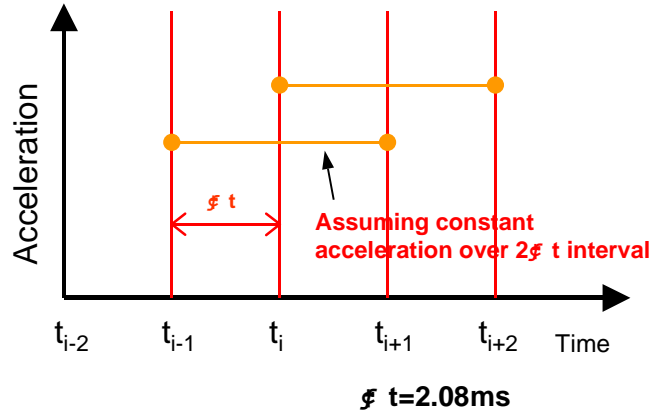


Figure 2: Assumption of acceleration in the central difference method

## Multi-axial control

Most of conventional hybrid experiments use one-axial control systems. Multi-axial real-time hybrid vibration system [Momoi, et al., 1997] is employed in the present study. Figure 3 shows the concept of multi-axial hybrid vibration experiment system. The reaction force  $F$  is measured and introduced into vibration response analysis. Then, the displacement at the center of the transfer plate at next step  $X(x, z, \theta)$  is calculated. In order to realize this displacement, three actuators yield displacements  $l_1, l_2$  and  $l_3$ , as shown in Figure 4.

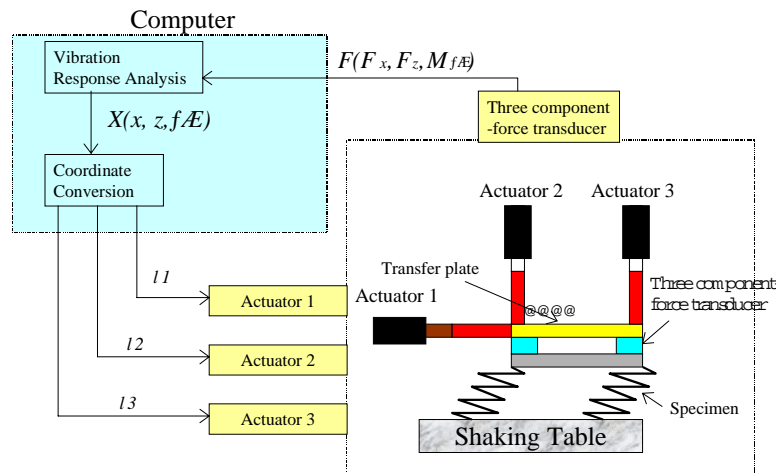


Figure 3: Concept of multi-axial hybrid vibration experiment system

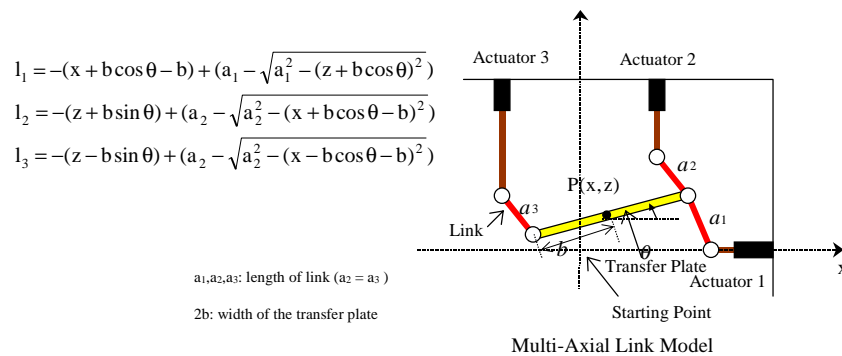


Figure 4: Method of multi-axial calculation

## Interlocking Experiment

In the previous study [Tamura and Kobayashi, 1998], we directly inputted the measured acceleration of the shaking table to the numerical computation part of a hybrid experiment for interlocking the numerical calculation and the shaking table test. This caused divergent phenomenon in some cases because the vibration of the the hybrid experiment apparatus interfered with the control of shaking table. In the present study, we use the control signal of shaking table for numerical analysis instead of the measured acceleration of shaking table.

## Inertia Force Modification

To attach a specimen to the hybrid vibration experiment apparatus, it is necessary to install the spacer between the specimen and the three component-force transducer, which results in that the inertia force due to weight of the spacer is included in the measured reaction force. To remove the effect of inertia force of the spacer, the following equation is here introduced:

$$\begin{aligned} f_{sx}' &= f_{sx} - M \times A_{sx} \\ f_{sz}' &= f_{sz} - M \times A_{sz} \end{aligned} \quad (4)$$

where,  $f_{sx}'$  and  $f_{sz}'$  are the modified loads,  $f_{sx}$  and  $f_{sz}$  are loads measured by the three component-force transducer,  $A_{sx}$  and  $A_{sz}$  are the acceleration measured by the accelerometer under the three component-force transducer, and  $M$  is the weight of spacer.

## 2. EXPERIMENT MODELS AND CASES

In order to demonstrate the validity of real-time hybrid vibration experiment, both real-time hybrid vibration experiments and conventional experiments with a whole structure model were conducted, and the results were compared.

Two types of original structures were employed in experiments. Type 1 is a concrete slab model which is supported by coil springs. In the experiment, we connected two slabs rigidly to move as one body. Type 2 consists of a 2-story slabs supported by rubber bearings and coil springs. Their conceptual views are presented in Figure 1. The slab part consists of H-shaped beams and infilled concrete. Using coil springs makes the motion of specimen as 2-dimensional and 3-degrees-of-freedom. The stiffness of coil springs and the weight of slabs were determined in advance by numerical analysis to yield the appropriate natural frequency for experiments.

**Table 1: Test Cases (Type 1)**

| Case Number | Input Motion                                       | Input Level | Duration |
|-------------|--|-------------|----------|
| Case 1      | 5 cycles of horizontal sinusoidal waves (f 1.32Hz) | 40 gal      | 20 s     |
| Case 2      | 5 cycles of vertical sinusoidal waves (f 2.10Hz)   | 50 gal      | 20 s     |
| Case 3      | JMA Kobe Record (Ns Comp)                          | 150 gal     | 30 s     |
| Case 4      | Port Island Kobe Record (Ns Comp)                  | 120 gal     | 30 s     |
| Case 5      | Elcentro Record (Ns Comp)                          | 120gal      | 45 s     |

**Table 2: Test Cases (Type 2)**

| Case Number | Input Motion                                       | Input Level | Duration |
|-------------|--|-------------|----------|
| Case 6      | 5 cycles of horizontal sinusoidal waves (f 1.17Hz) | 30 gal      | 20 s     |
| Case 7      | 5 cycles of vertical sinusoidal waves (f 2.05Hz)   | 40 gal      | 20 s     |
| Case 8      | JMA Kobe Record (Ns Comp)                          | 100 gal     | 30 s     |
| Case 9      | Port Island Kobe Record (Ns Comp)                  | 100 gal     | 30 s     |
| Case 10     | Elcentro Record (Ns Comp)                          | 100gal      | 45 s     |

In order to find the fundamental natural frequency of test specimen, both horizontal and vertical random shaking tests were carried out with the original structures. The horizontal and vertical fundamental natural frequencies of type 1 model are 1.32 Hz and 2.10 Hz, and those of type 2 model are 1.17 Hz and 2.05 Hz.

Test cases of hybrid vibration experiments are listed in Table 1 and Table 2. In the hybrid vibration experiment for type 1 model, the mass, stiffness and damping over coil springs were numerically modeled. In the hybrid vibration experiment for type 2 model, the mass, stiffness and damping of the upper level and the mass of the lower level were numerically modeled, as shown in Figure 5. Besides the hybrid vibration experiments, conventional experiments with the whole structure were also conducted, and the results of hybrid vibration experiments and conventional experiments were compared.

Input motions employed for experiments were five cycles of sinusoidal wave with the frequency that corresponds to the horizontal or vertical fundamental natural frequency of the whole structure, and the strong ground motion recorded in the past as shown Table 1 and Table 2. The maximum peak acceleration was variously changed in experiments.

## NUMERICAL MODELS FOR HYBRID VIBRATION EXPERIMENTS

### Numerical model

Numerical models for hybrid vibration experiments are shown in Figure 5, and equations of motions for numerical analysis are described for type 1 and type 2 models as follows:

#### Type 1

$$M\ddot{x} + C\dot{x} + Kx = p + q$$

$$x = \begin{bmatrix} x \\ z \\ f \\ \frac{E}{y} \end{bmatrix}, M = \begin{bmatrix} m & 0 & -mH \\ 0 & m & 0 \\ -mH & 0 & J \end{bmatrix}, K = \begin{bmatrix} 0 & 0 & 0 \\ 0 & 0 & 0 \\ 0 & 0 & -mgH \end{bmatrix}, p = \begin{bmatrix} F_x \\ F_z \\ M_y \end{bmatrix}, q = - \begin{bmatrix} m & 0 \\ 0 & m \\ -mH & 0 \end{bmatrix} \begin{bmatrix} \ddot{x}_g \\ g + \ddot{z}_g \end{bmatrix} \quad (5)$$

#### Type 2

$$M\ddot{x} + C\dot{x} + Kx = p + q$$

$$x = \begin{bmatrix} x \\ z \\ f \\ \frac{E}{y} \\ u \end{bmatrix}, M = \begin{bmatrix} m_1 + m_2 & 0 & -m_1H_1 - m_2H_2 & m_2 \\ 0 & m_1 + m_2 & 0 & 0 \\ -m_1H_1 - m_2H_2 & 0 & J & -m_2H_2 \\ m_2 & 0 & -m_2H_2 & m_2 \end{bmatrix}, K = \begin{bmatrix} 0 & 0 & 0 & 0 \\ 0 & 0 & 0 & 0 \\ 0 & 0 & -m_1gH_1 - m_2gH_2 & m_2g \\ 0 & 0 & m_2g & k_u \end{bmatrix}, p = \begin{bmatrix} F_x \\ F_z \\ M_y \\ 0 \end{bmatrix}, q = - \begin{bmatrix} m_1 + m_2 & 0 \\ 0 & m_1 + m_2 \\ -m_1H_1 - m_2H_2 & 0 \\ m_2 & 0 \end{bmatrix} \begin{bmatrix} \ddot{x}_g \\ g + \ddot{z}_g \end{bmatrix} \quad (6)$$

$g$  in eq (5) and (6) represents the gravitational acceleration, and the mass, damping and stiffness matrices are shown in the following sections.

### Mass Matrix

The mass matrix consists of weight of numerical part  $m$ , height of the center of gravity  $H$  and inertia moment  $J$  ( $=mH^2 + I$ ,  $I$ : inertia moment around the center of gravity), which are shown in eqs. (5) and (6).

#### Type 1

The weight  $m_i$ , the height of the center of gravity  $H_i$  and the inertia moment around the center of gravity  $I_i$  for each structural part were calculated from the design drawing of the specimen. From those values  $m$ ,  $H$  and  $J$  of the whole numerical mode are obtained as

$$m = \sum m_i, H = \frac{\sum m_i H_i}{m}, J = \sum (m_i H_i^2 + I_i) \quad (7)$$

#### Type 2

In addition to the mass of slabs, that of rubber bearings was also considered.

### Damping Matrix

#### Type 1

The damping was ignored because the damping of the original structure part that is numerically modeled is small.

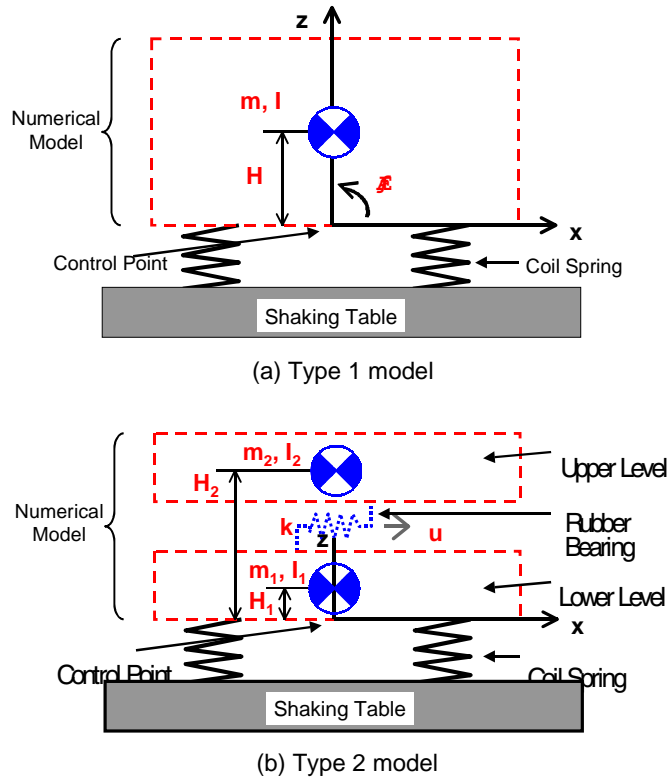


**Figure 5: Numerical model for hybrid vibration experiment**

**Type 2**

The damping of rubber bearings were considered. The damping matrix was estimated from the damping ratio to the critical  $\zeta=0.026$ , which was obtained by free vibration tests, and the relationship  $C=\beta K(\beta=2\zeta/\omega)$ .

**5.4 Stiffness Matrix**

**Type 1**

$m$  and  $h$  were calculated similar to the case of  $m$  and  $h$  in the mass matrix.

**Type 2**

The stiffness of rubber bearings were considered. The stiffness coefficient was determined as  $2.6 \times 10^6 \text{N/m}$  based on forced vibration tests.

**EXPERIMENT RESULTS**

Figures 6 and 7 compare acceleration time histories of the control point (Figure 5) in hybrid vibration experiments and conventional shaking table tests with the whole structure. Results are shown for Cases 1, 2, 4, 6, 7 and 9. The hybrid vibration experiment well reproduces both amplitude and phase of acceleration time history. Causes of slight error between real-time hybrid vibration experiments and conventional shaking table tests may exist in:

- (1) Detection error by the three component-force transducer:

Since the reaction force generated in the experiments was small and reached several-percent of the rated capacity of transducer, there existed certain error in load measurement.

- (2) Difference of the restricting condition:

Although the freedom of specimen was 3-dimensional and 6-degrees in conventional shaking table tests, it was restricted to 2-dimensional and 3-degrees-of-freedom in hybrid vibration experiment. For example, slight movement around the vertical axis was generated in conventional shaking table test, and this might affect the experiment result.

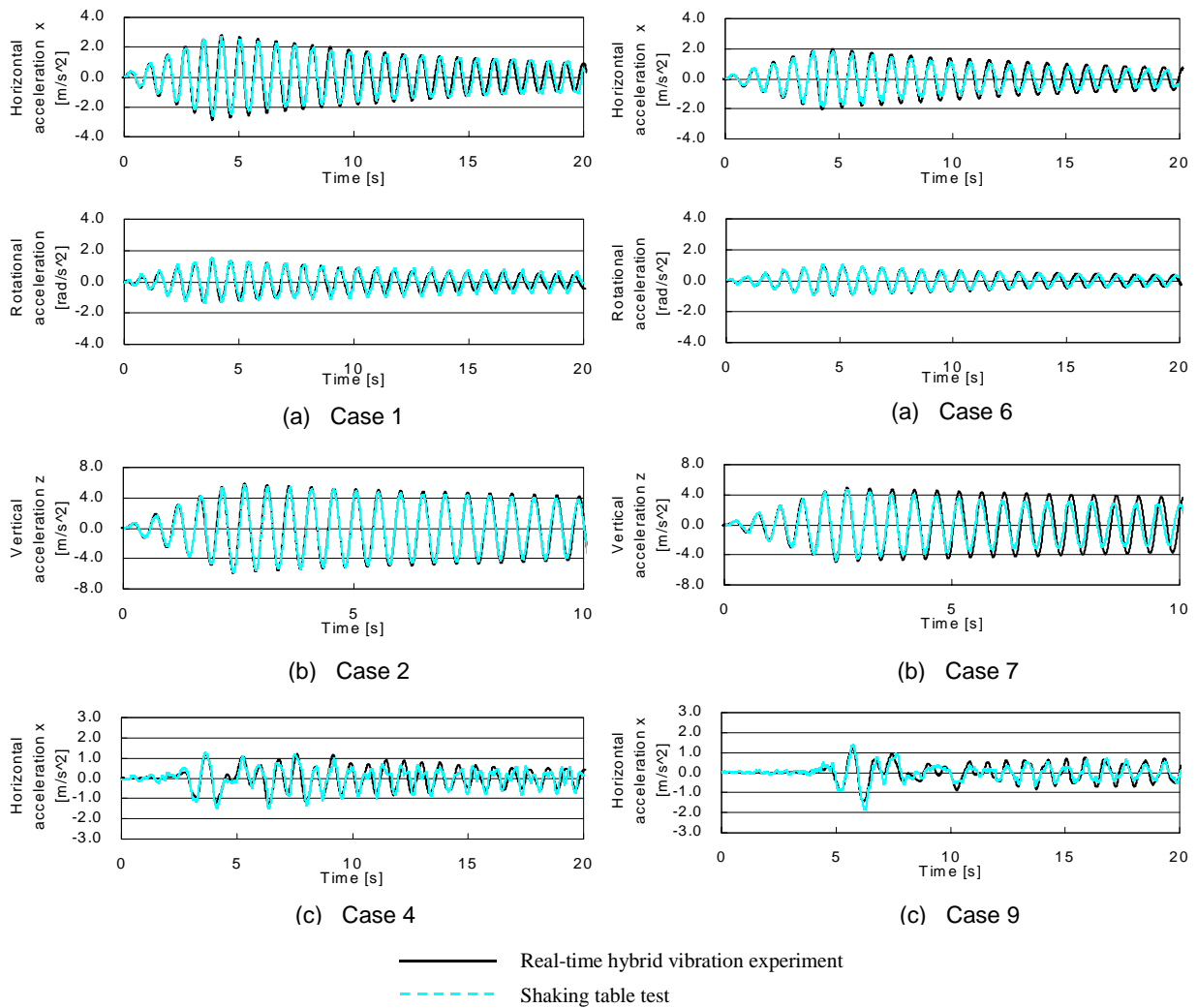


**Figure 7: Acceleration time histories of the control point (Type 1 model)**

**Figure 8: Acceleration time histories of the control point (Type 2 model)**

## CONCLUSIONS

We employed actuator delay compensation for the real-time experiment, and contrived multi-axial control for multi-degrees of freedom experiment. The real-time hybrid vibration experiment well reproduces seismic behavior of the 2-dimensional and 3-degrees-of-freedom model and the validity of experiment is confirmed.

## REFERENCES

1. Horiuchi, T., Nakagawa, M., Sugano, M. and Konno, T. (1996), "Development of a Real-Time Hybrid Experimental System with Actuator Delay Compensation", *Proc. 11th World Conference on Earthquake Engineering*
2. Momoi, Y., Horiuchi, T., Umekita, K., Inoue, M. and Sugano, M. (1997), "Development of Real-Time Hybrid Seismic Experimental System using Multiple-Axis Shaking Device", *Proc. 5th Symposium on Motion and Vibration Control, JSCE*, pp 415-418. (in Japanese)
3. Tamura, K. and Kobayashi, H. (1998), "Real-time Hybrid Vibration Experiment with a 2-Degrees-of-Freedom Model", *Proc. 30th Joint Meeting, Panel on Wind and Seismic Effects, UJNR*, pp41-49.
4. Umekita, K. et al. (1997), "Development of C Language Library for Super Real-Time Controller (SRC) for Real-Time Hybrid Seismic Testing System with Three-dimensional-in-plane Excitation", *Proc. 40th Japan Joint Automatic Control Conference*, pp 393-396. (in Japanese)